Available online at www.sciencedirect.com
SCIENCE DIRECT
Biomaterials 27 (2006) 2898–2906
Biomaterials
www.elsevier.com/locate/biomaterials

Use of thermodynamic parameters for design of double-walled microsphere fabrication methods

Emily J. Pollauf[a], Daniel W. Pack[a,b,*]

[a]Department of Chemical and Biomolecular Engineering, University of Illinois, Urbana, IL, USA
[b]Department of Bioengineering, University of Illinois, Urbana, IL, USA

Received 26 August 2005; accepted 6 January 2006

Abstract

Double-walled microspheres (DWMS), with drug localized to the particle core, present a promising route for control of drug release rates, for example, by varying the degradation rate or erosion mechanism of the polymer used to form the shell or the thickness of the shell. DWMS are often difficult to fabricate, however. Thermodynamic descriptions for polymer–polymer immiscibility, drug distribution between phases and polymer–solution spreading coefficient provide predictions of appropriate solvents and polymer concentrations for efficiently producing well-formed DWMS. As an example, thermodynamic parameters for a polyphosphoester/poly(D,L-lactide-*co*-glycolide) (PLG) DWMS system, encapsulating piroxicam, have been calculated and the predictions tested experimentally. Appropriate choices of solvents and initial polymer concentrations resulted in DWMS with the desired polyphosphoester shells and piroxicam located selectively in PLG cores.

Keywords: Microcapsules; Double-walled microspheres; Microencapsulation; Controlled drug release; Piroxicam

1. Introduction

Microcapsule drug delivery devices may consist of polymer shells surrounding oil, aqueous or solid cores loaded with the drug [1–5]. The addition of a second polymer layer to a biodegradable polymeric microsphere may provide the opportunity to tune release rates through selection of the appropriate core and shell polymer chemistries, which control degradation rates, erosion mechanisms and water penetration to the core [6–10]. Selective location of drug to the core or shell, or of two drugs to the core and shell, respectively, can result in complex release profiles [11,12]. Double-walled microspheres (DWMS), comprising a core of one polymer and a shell of a second (or the same) polymer, are thus particularly attractive drug delivery vehicles for many applications [9,12–16].

The formation of DWMS with selective polymer and drug locations depends on the thermodynamic interactions of the polymers and drugs. For example, difficulties in forming well-defined core and shell regions often can be related to polymer–polymer miscibility. Also, thermodynamics can dictate that one polymer will preferentially spread on the other (as a result of the polymers' and polymer solutions' interfacial tensions) [17]. Additionally, drugs will typically exhibit a preference for localization within one of the two polymers [18].

DWMS have been fabricated using emulsion/extraction methods analogous to those commonly used for microsphere fabrication [6–9,18] or by coating solid microspheres [19]. Using these conventional methods, partial encapsulation (i.e. the shell polymer does not completely engulf the core) is often observed if experimental conditions are not carefully chosen. The emulsion/extraction fabrication processes can also be limited by the thermodynamically favorable distribution of one polymer as the shell and the other as the core since the two polymers start in a homogeneous solution [13]. In order to change the final polymer distribution, it is sometimes necessary to adjust

*Corresponding author. Department of Chemical and Biomolecular Engineering, University of Illinois, Urbana, IL, USA.
Tel.: +1 217 244 2816; fax: +1 217 333 5052.
E-mail address: dpack@uiuc.edu (D.W. Pack).

0142-9612/$ - see front matter © 2006 Elsevier Ltd. All rights reserved.
doi:10.1016/j.biomaterials.2006.01.005

the solvent extraction rates to kinetically trap the DWMS in a non-equilibrium configuration. Optimizing parameters for all of these considerations usually leads to compromises in the final product.

Several types of DWMS have been reported previously. For example, Yang et al. described formation of core–shell particles with poly(D,L-lactide-*co*-glycolide) (PLG) shells encapsulating polyorthoester (POE) cores at various POE:PLG ratios [9]. Similarly, because poly(L-lactide) (PLL) preferentially spreads on poly(1,3-bis(*p*-carboxyphenoxy)propane-*co*-sebacic anhydride)20:80 (P(CPP:SA)20:80), DWMS can be formed using an emulsion with solutions of the two polymers at equal concentration [6,14,20]. Both the POE/PLG and PLL/P(CPP:SA)20:80 systems relied on the immiscibility of the two polymers to promote phase separation. In cases where miscibility of the polymers is expected, concentrations at which polymer–solution phase separation does occur can sometimes be experimentally determined with cloud point measurements. For example, polylactide/PLG DWMS have previously been fabricated at concentrations above experimentally determined critical concentrations [11,18].

A different approach for particle fabrication, known as precision particle fabrication (PPF) technology, employs a series of annular nozzles to create a compound jet, which is subsequently broken into uniform droplets by acoustic excitation [21,22]. An advantage of the PPF method is that the core and shell polymer streams are initially positioned in the desired final configuration by the nozzle system; the core polymer forms the innermost stream exiting the nozzle, while the shell polymer forms the middle annular stream with a non-solvent carrier as the outermost stream. Since the polymer solutions are not in contact until they exit the nozzle, polymer mixing is limited to diffusion between the laminar streams or within the nascent droplets as they harden. Such effects, even for miscible or partially miscible polymers, are expected to be slow and could be further minimized by the use of a fast-extracting solvent. The separation of the two polymer streams allows for more freedom in selecting appropriate solvents and concentrations for each stream individually. For example, PPF has been used to form polylactide(PLG) DWMS in which the drug release rate (from the core) depends strongly on the shell thickness [15,16].

Selection of solvents and concentrations for specific polymer–polymer–drug combinations can be aided by thermodynamic calculation of polymer–polymer phase separation, polymer–solution spreading coefficients and drug distribution within the system. These calculations rely on the use of the solubility parameter, δ, to predict polymer, drug and solvent interactions in two-polymer DWMS systems. Building on the theoretical results, methods to achieve the desired DWMS properties can be designed and experimentally tested.

In the studies reported here, DWMS comprising polyphosphoester (polilactofate, PLF) shells surrounding PLG cores were used to encapsulate a model small molecule, piroxicam. Because PLF and PLG are very similar materials, careful choice of fabrication parameters is required to produce DWMS with drug selectively localized to the core. The effects of two different solvents, methylene chloride (DCM) and ethyl acetate (EtAc) and initial polymer solution concentrations on the capsule morphology, drug loading, and particle size were investigated. Comparison of experimental results with predictions based on thermodynamic considerations sheds light on the role of polymer, drug and solvent interactions in DWMS systems.

2. Materials and methods

2.1. Materials

PLG (50:50 copolymer, 0.39 dL/g in hexafluoroisopropanol) was purchased from Birmingham Polymers. PLF was a gift from Guilford Pharmaceuticals, Inc. Piroxicam was donated by Dong Wha Pharmaceuticals (Seoul, South Korea). Poly(vinyl alcohol) (PVA, 24 kDa, 88% hydrolyzed) was purchased from Polysciences (Warrington, PA). DCM, EtAc and HPLC-grade chloroform were obtained from Fisher Scientific (Fairlawn, NJ). Unless otherwise specified, all solvents were reagent grade.

2.2. Molecular weight analysis

Gel permeation chromatography (GPC) was used to determine polymer molecular weights. The system consisted of a Waters 1515 HPLC pump, Waters 715plus autoinjector, and Waters 410 differential refractive index detector. Separation was performed in linear Styragel HR 3, HR 4 and HR 4E columns from Waters (Milford, MA) at 40 °C. Polystyrene standards (ten molecular weights from 580 to 299,400) from Polymer Laboratories (Amherst, MA) were used to generate the calibration curve at concentrations of 1 mg/mL. The semilog calibration curve of molecular weight versus elution volume was linear with $R^2 = 0.995$. HPLC-grade chloroform at a flow rate of 1 mL/min was used as the mobile phase. Samples of each polymer were dissolved in HPLC-grade chloroform at a concentration of 1 mg/mL. Molecular weights and polydispersities are reported as the average of two measurements.

2.3. Contact angle measurement

Polymer films for contact angle measurement were prepared by dissolving 3% w/v polymer in DCM. A 0.5-mL droplet of this solution was spread on a glass slide, and the solvent allowed to evaporate. Advancing contact angles for water and methylene iodide on the polymer films were measured using a Gaertner goniometer-microscope. All reported values are the average of at least four measurements per sample.

2.4. Polymer–polymer miscibility

To determine the total polymer concentration at which two polymers became immiscible, a total of 400 mg of the two polymers were weighed in the selected mass ratio. Eight milliliters of solvent was added to create a 10% w/v solution. After complete dissolution of the polymers was observed, the solution was transferred to a 10 mL graduated cylinder, open to the atmosphere and at room temperature. The initial volume was recorded, and solvent was allowed to evaporate. When cloudiness became apparent in the solution, the volume of solution was recorded. It was assumed that only solvent losses had contributed to the volume change. The cloud point concentration was taken to be the critical concentration at which the two polymers became immiscible (assuming both polymers were still individually soluble at that concentration).

2.5. DWMS fabrication

We employed the precision particle fabrication technology [21] with a triple nozzle [10,15,16,23] to create DWMS. The nozzle system generated core and annular polymer solution streams surrounded by an outermost carrier fluid (0.5% PVA in deionized water). Most batches of particles employed core solutions of 40% w/v PLG and shell solutions of 3% w/v PLF in the specified solvents. Two polymer solutions of equal volume were made for one batch above the critical concentration: one with 25% w/v PLG and 10% w/w piroxicam, the other with 25% w/v PLF, both in EtAc. The liquid jet exiting the nozzle was broken into uniform droplets by acoustic excitation and collected in a stirred bath of 900 mL of 0.5% PVA solution. After collection, the bath was stirred for several hours (3 h for DCM solvents, 24 h for EtAc) to allow for complete solvent extraction from the spheres. DWMS were washed with 900 mL of deionized water in a vacuum filtration system prior to lyophilization for 48 h. Samples were stored until use in a −20 °C freezer with desiccant.

2.6. Size distributions

The size distributions of hardened DWMS were determined using a Beckman Multisizer 3 with a 280 μm aperture. The particles were suspended in Isoton II with two drops of dispersant Type A. At least 5000 spheres were measured for every sample.

2.7. Drug loading

DWMS samples were accurately weighed (2–4 mg) and digested in 1 mL of 0.2 M sodium hydroxide for 1 week at 37 °C. The absorbance was measured with a Cary Eclipse UV–Visible Spectrometer at 350 nm. Drug-free polymer microspheres were digested in the same manner and scans were run from 200 to 1100 nm to verify that no absorption due to the polymer occurred at the measurement wavelength. Absorbances were converted to drug concentration using a standard curve prepared using known concentrations of piroxicam in 0.2 M NaOH. Loading is defined as mass of drug per mass of polymer, presented as a percentage. Encapsulation efficiency (e.e.) was calculated as the ratio of measured loading to theoretical loading.

2.8. Microscopy

Optical and fluorescent images of the particles were obtained using an Olympus Fluoview FV300 Laser Scanning Biological Microscope. A helium–neon laser was used to fluorescently excite piroxicam. Core encapsulation efficiencies were determined from optical micrographs. Images of several hundred particles were captured at the particle midline. Visual observation was used to determine the number of particles with encapsulated cores relative to the total number of particles imaged.

The exterior and interior morphologies of the samples were imaged using a Hitachi S-4700 scanning electron microscope (SEM). A razor blade was used to cross-section frozen particles dried on metal sample holders. The samples were sputter coated for 45 s at 20 mA using an Emitech K-575 Sputter Coater with a gold–palladium target. Images were obtained at 5 kV.

3. Theory

The solubility parameter of a species is based on the thermodynamics of mixing [24] and can be defined as the square root of the cohesive energy density (CED):

$$\delta = \sqrt{\mathrm{CED}} = \sqrt{\frac{\Delta E_\mathrm{v}}{V_\mathrm{m}}}, \tag{1}$$

where ΔE_v is the energy of vaporization and V_m is the molar volume. CED is the amount of energy necessary to separate the atoms or molecules of a material to a distance where they experience no interactions. The solubility parameter description has been extended to apply to polar species by dividing the total solubility parameter, δ_t, into a three-dimensional, or Hansen, solubility parameter comprising three component terms: δ_d due to dispersive forces, δ_p to polar interactions and δ_h to hydrogen bonding [25].

Solubility parameters can be calculated using group contribution methods based on a material's structure and assuming the total parameter for a molecule is a sum of the values for each constituent group. For partial solubility parameters the group contribution equations are given by van Krevelen [26] as

$$\delta_\mathrm{d} = \frac{\sum_i F_{\mathrm{d}i}}{V_\mathrm{m}}, \tag{2}$$

$$\delta_\mathrm{p} = \frac{\sqrt{\sum_i F_{\mathrm{p}i}^2}}{V_\mathrm{m}}, \tag{3}$$

$$\delta_\mathrm{h} = \sqrt{\frac{\sum_i E_{\mathrm{h}i}}{V_\mathrm{m}}}, \tag{4}$$

where $F_{\mathrm{d}i}$, $F_{\mathrm{p}i}$ and $E_{\mathrm{h}i}$ are the group contributions for δ_d, δ_p and δ_h, respectively and V_m is the molar volume, also calculated by group contribution theory. The total solubility parameter for a compound is given by the root mean square of the partial parameters. For polymers, all calculations are based on the monomer repeat unit. Contributions for the individual groups $F_{\mathrm{d}i}$, $F_{\mathrm{p}i}$ and $E_{\mathrm{h}i}$ have been published by van Krevelen [26]. The most complete (although less accurate) set of total solubility parameter groups has been assembled by Fedors [27] and is often used for calculations of V_m.

The solubility parameter has found application in the classic Flory–Huggins theory of interaction parameters for polymers [28]. The theory has been examined for extension to ternary systems by Scott [24,29,30]. Of particular interest in DWMS formation is the description of polymer–polymer–solvent systems [29]. The critical solvent volume fraction for immiscibility and phase separation of the two polymers in the ternary system is given by

$$\phi_{0\mathrm{crit}} = 1 - \frac{1}{2\chi_{12}}\left(\frac{1}{\sqrt{x_1}} + \frac{1}{\sqrt{x_2}}\right)^2. \tag{5}$$

χ_{12} in this equation is the Flory–Huggins interaction parameter for the system [28] and x_i is the number-averaged degree of polymerization for each polymer corrected by the ratio of the polymer-to-solvent molar volumes.

Solubility parameters can also be used with distribution theory [31] to predict the preferential location of a solute between two phases with

$$\log\left(\frac{[X_1]}{[X_2]}\right) = V_S \frac{(\delta_s - \delta_2)^2 - (\delta_1 - \delta_s)^2}{2.3\,RT}, \quad (6)$$

where $[X_i]$ is the mole fraction of the solute in each phase, V_s is the molar volume of the solute, δ_i is the solubility parameter of the solute (s) and phases (1 or 2), R is the gas constant and T is the absolute temperature. Eq. (6) can be simplified to consider only the solubility parameter differences, as a means of indicating the preferred polymer phase [18]. For positive values of the solubility parameter differences, the drug is predicted to prefer polymer 1 and for negative values polymer 2. For values near zero, the drug is expected to prefer the interface of the polymers. A larger difference indicates a stronger preference for one phase versus the other.

Fabrication of DWMS is also dependent on one polymer fully spreading over the other. The engulfment is described by spreading coefficient theory as developed by Harkins [17] for a liquid spreading on a solid surface. Torza and Mason [32] extended Harkins' theory to systems of two immiscible phases suspended in a third immiscible phase. Eq. (7) allows calculation of the spreading coefficient for each phase from the interfacial tensions between the phases, γ_{12}, γ_{23} and γ_{13}:

$$\lambda_{ij} = \gamma_{jk} - \gamma_{ij} - \gamma_{ik}. \quad (7)$$

Only three independent spreading coefficients exist for the three-phase system, and by defining phase 2 as the continuous phase and specifying phase 1 such that $\gamma_{12} > \gamma_{32}$ (i.e. $\lambda_{12} < 0$), it is found that only three possible combinations of the spreading coefficients exist (Table 1). By Harkins' definition, a positive spreading coefficient leads to spreading of phase i on phase j. Therefore, the three resulting possibilities are total encapsulation of phase 1 within phase 3 (Case A), partial engulfment leading to an "acorn" morphology (Case B) and complete separation of phases 1 and 3 (Case C). All three situations have been found experimentally, and spreading coefficient theory has been quite accurate in predicting small molecule and polymer spreading both in solution and the melt [8,13,14,32,33].

The interfacial tensions in Eq. (7) are calculated, with the component surface tension, according to

$$\gamma_{12} = \left(\sqrt{\gamma_1} - \sqrt{\gamma_2}\right)^2. \quad (8)$$

Table 1
Prediction of final DWMS configuration based on spreading coefficients

Total encapsulation (case A)	Partial encapsulation (case B)	No engulfment (case C)
$\lambda_{12} < 0$	$\lambda_{12} < 0$	$\lambda_{12} < 0$
$\lambda_{23} < 0$	$\lambda_{23} < 0$	$\lambda_{23} > 0$
$\lambda_{31} > 0$	$\lambda_{31} < 0$	$\lambda_{31} < 0$

An experimental determination of polymer surface tensions can be obtained from contact angle measurements. Following the procedure of Wu [34], the contact angle of two different solvents (one polar, the other strongly dispersive) with a solid polymer film is measured. Use of the harmonic-mean equation has been found to be most accurate for polymers [26,34]. Simultaneously solving the harmonic-mean version of Young's equation using contact angles for the polymer with each of the two liquids will give the polymer components of the surface tension:

$$(1 + \cos\theta_i)\gamma_i = 4\left(\frac{\gamma_i^p \gamma_s^p}{\gamma_i^p + \gamma_s^p} + \frac{\gamma_i^d \gamma_s^d}{\gamma_i^d + \gamma_s^d}\right), \quad (9)$$

where i refers to the liquid, s to the solid polymer film and θ_i is the contact angle between the polymer and solvent. Simple addition of the polar and harmonic components gives the overall polymer surface tension.

4. Results and discussion

4.1. Thermodynamic predictions

For each polymer studied here, the number-averaged molecular weight (M_N) and number-averaged degree of polymerization, x_N were measured by GPC (Table 2). Accurate group contributions are available for "rubbery" and "glassy" polymers to calculate the molar volume, and thus, the density [26]. If a polymer is above its glass transition temperature (T_g) at room temperature, it is considered a "rubbery" polymer for the purposes of these calculations. A polymer below its T_g at room temperature is a "glassy" polymer. The phosphorus group contributions for PLF could not be obtained from the rubbery and glassy polymer molar volume tables, so Fedors' data [27] was assumed for this group. For PLG and the remainder of the groups in PLF, the calculations were performed for glassy polymers, since both are below their T_g at room temperature [35,36]. The partial and total solubility parameters for the polymers have been calculated by group contribution methods [26] using Eqs. (2)–(4) (Table 2). These calculated solubility parameters are 1.3–3.1% higher than previously reported experimental values for PLG and piroxicam [1,37]. Solvent solubility parameters were obtained from the literature [38]. The polymer surface tensions (Table 3) were calculated from experimental measurements of selected polymer contact angles with

Table 2
Molar volumes and solubility parameters (components and total) for polymers and drug calculated using group contributions

Species	$\overline{M}_N$ (Da)	$\overline{x}_N$	V_m (cm^3/mol)	δ_d	δ_p	δ_h	δ_t
PLG	14,000	216	47.6	16.3	10.3	12.2	22.8
PLF	43,200	577	58.3	15.9	8.8	11.1	21.3
Piroxicam	n/a	n/a	189.7	23.3	8.3	14.7	28.8

Solubility parameters are in MPa$^{0.5}$.

Table 3
Contact angles and component surface tensions for polymers

Polymer	θ_{water}	θ_{DCM}	γ^p(mJ/m^2)	γ^d (mJ/m^2)
PLG (0.39 dL/g)	69.3	44.4	27.7	16.3
PLF	74.0	40.7	30.1	13.2

water and methylene iodide using a harmonic mean of Young's equation. The polar and dispersive components of the liquid surface tensions were obtained from Wu [34].

4.1.1. Polymer–polymer immiscibility

Polymer–polymer immiscibility is critical in creating well-defined core and shell regions within a DWMS. If complete polymer phase separation does not occur, drug release and polymer degradation may be significantly different than expected for a true DWMS morphology. Using Scott's equations for polymer–polymer immiscibility in a common solvent, PLG and PLF are predicted to be immiscible above a total polymer concentration of 16.5% w/v. (The calculation for critical total polymer concentration is independent of the solvent.) Experimental measurements of PLF/PLG miscibility in DCM and EtAc show the critical concentration for immiscibility to be solvent dependent and higher than the calculated value in both cases (26.7% and 20.0% w/v for DCM and EtAc, respectively). The higher experimental values may be due to late detection of the cloud point, since direct visual observation was the only tool employed. Thus, although lower concentrations may also be allowable, to ensure phase separation, the total polymer concentration should be maintained greater than 27% w/v for DCM, or 20% w/v for EtAc solvents.

4.1.2. Drug partitioning

Drug distribution between two polymer phases is of critical concern for loading of drug into the core. The calculation proposed by Matsumoto et al. [18] on the basis of distribution theory captures some overall aspects of drug distribution, but has the critical limitation of being polymer-concentration dependent. As a consequence, the drug distribution cannot be predicted as the particles harden, since rates of solvent extraction are unknown and difficult to predict or measure. To obtain a better understanding of possible drug distributions within DWMS, both the preferred distribution at the starting solvent concentrations (3% w/v shell solution, 40% w/v core solution) and the distribution with no solvent present in the system were examined. The calculations for the DWMS with piroxicam captured a range of possible solvent configurations with DCM and EtAc as the solvents.

Strong differences in drug distribution were predicted between the solvent configurations. A positive value indicates a preference of the drug to the PLG phase, while a negative value indicates a preference to PLF (Fig. 1A). When no solvent is present, piroxicam is predicted to favor

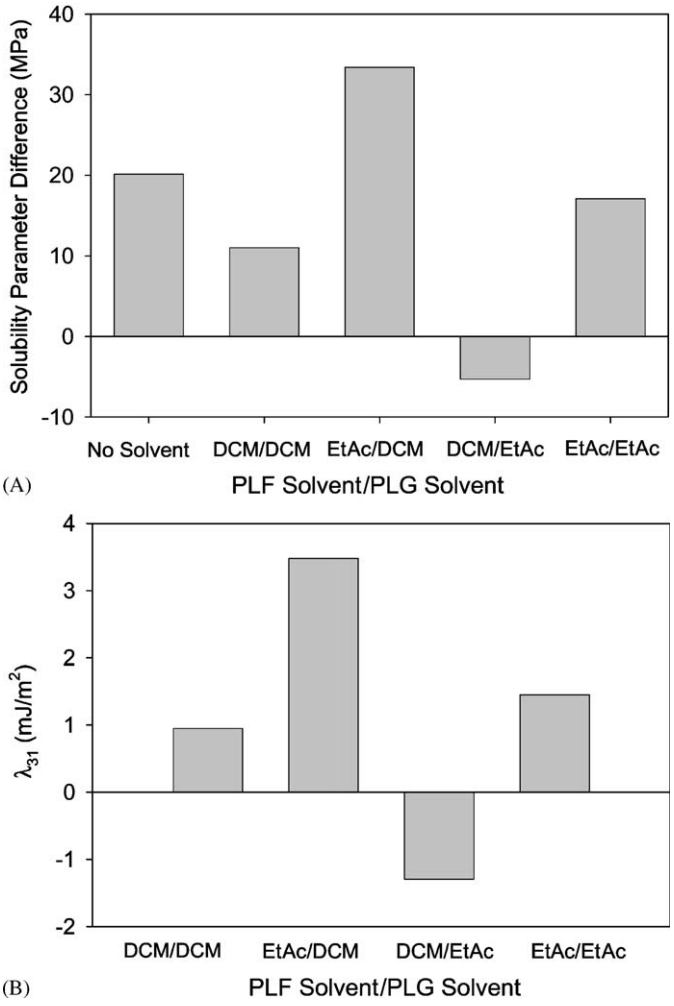

Fig. 1. (A) Calculated solubility parameter differences between PLF, PLG and piroxicam in DCM and EtAc solvents. (B) Calculated spreading coefficients (λ_{31}) for 3% w/v PLF and 20% w/v PLG (0.39 dL/g) in various solvent combinations.

PLG over PLF. Similarly, piroxicam prefers the PLG phase in the DCM/DCM, EtAc/DCM and EtAc/EtAc systems; the strongest preference of the drug for PLG is observed with EtAc/DCM. (The fabrication conditions will be referred to as "shell solvent"/"core solvent"; for example, DCM/EtAc indicates particles fabricated using PLF dissolved in DCM as the shell phase and PLG in EtAc as the core phase. In all particles, PLF forms the shell and PLG the core.) In the DCM/EtAc system, however, piroxicam slightly preferred the PLF phase. Since our goal was to encapsulate piroxicam in PLG cores, the use of an EtAc/DCM system appears to be the most promising.

4.1.3. Polymer spreading

Spreading coefficients can be used to predict the encapsulation of one polymer phase within another. As with the drug distribution, the spreading coefficient will change with time as the particles harden; i.e., as solvent is extracted, the polymer solution concentrations will change, altering the effective interfacial tensions. Again, the

spreading coefficients were calculated at the starting polymer concentrations and for the melt polymers (i.e., without solvent present) as an indirect estimation of the final configuration of the polymers after solvent extraction. The assumption of completely immiscible polymers also applies.

For the calculation of the spreading coefficients in solution, the method of Torza and Mason [32] was applied. The polymer–solution surface tensions were calculated from a volume-weighted average of the polymer and solvent values. The melt-phase polymer spreading was determined using Eq. (7) in its two-component form.

The PLF/PLG system illustrates the impact of initial solution concentrations. When equal concentrations (25% w/v) of the two polymers are used, PLF is weakly predicted to spread on PLG ($\lambda_{31} = 0.007$). If the PLF solution concentration is reduced to 3% w/v, then PLF is predicted to more readily spread on PLG ($\lambda_{31} = 1.8$). If the concentration of the PLG core is further increased, the value of λ_{31} continues to increase.

Using a 3% w/v concentration to induce PLF spreading on PLG (20% w/v), situations with mixed solvents can then be considered for improved DWMS formation. Combinations of EtAc and DCM in PLF and PLG solutions yield different spreading scenarios (Fig. 1B). The best spreading of PLF on PLG will come from the largest positive value, in this case for EtAc/DCM. The negative λ_{31} value for DCM/EtAc does not indicate a lack of encapsulation. Rather, in order to maintain $\lambda_{12} < 0$ as required by spreading coefficient theory specifications, the value had to be calculated for PLG spreading on PLF. This did give a positive value, which has been plotted as negative here to indicate the reversal in the spreading polymer.

4.1.4. Summary of predictions

PLF/PLG polymer–polymer immiscibility occurs for total polymer concentrations above 27% w/v based on thermodynamic parameter calculations. Spreading of PLF on PLG, however, is predicted to be much stronger with a shell concentration of 3% w/v and at least a 20% w/v core solution. Further, both (i) strong partitioning of piroxicam to the PLG core and (ii) spreading of the PLF shell on a PLG core are predicted to occur with the EtAc/DCM system. Thus, a low concentration of PLF in EtAc and a higher concentration of PLG in DCM (containing piroxicam) are expected to provide the best conditions for producing the desired DWMS.

4.2. Experimental DWMS formation

To test the validity of the thermodynamic calculations, microparticles were formed using the precision particle fabrication technology. Core- and shell-solvent combinations of EtAc and DCM were explored with 3% w/v shell and 40% w/v core solution concentrations. In addition, a batch of particles in which both the core and shell solutions were 25% w/v in EtAc was produced to investigate conditions above the experimentally determined critical total polymer concentration.

DCM is a popular solvent for particle fabrication due to its low boiling point and subsequently fast evaporation. Its low water solubility (1.6% w/w) means the primary microparticle hardening mechanism is by solvent evaporation from the collection bath. The increased water solubility of EtAc (8.7% w/w) allows a greater amount of solvent extraction. An increased extraction rate leads to faster removal of solvent from the nascent polymer droplets and faster hardening. However, with EtAc having a higher boiling point, evaporation of the solvent from the water bath will be significantly slower. The increased water solubility also means that more solvent will be present in the bath. Despite this offsetting extraction/evaporation interplay, a previous study has shown EtAc-based microspheres to harden faster than those formed with DCM solutions, at least for some drugs [39]. Work with EtAc has also shown higher drug encapsulation efficiencies to be an added benefit [39]. Since the DCM solvent in the collection bath led to decreased drug and core encapsulation efficiencies, EtAc's increased extraction rate may result in better core/shell formation.

4.2.1. DWMS characterization

Several batches of PLF(PLG) particles were fabricated using PPF, with different solvents used for the core and shell streams, as described above (Table 4). DWMS diameters ranged from 55 to 64 μm, with the DCM/DCM capsules being the smallest and most uniform and the EtAc/EtAc particles having the largest diameter and broadest distribution of diameters. In general, those

Table 4
Size, drug loading and encapsulation efficiency of PLF(PLG) DWMS as a function of core and shell solvent

Shell solvent, conc. (w/v) (PLF)	Core solvent, conc. (w/v) (PLG)	Average overall diameter (μm)	Standard deviation of size distribution (μm)	Drug loading (μg/mg)	Encapsulation efficiency (%)
DCM, 3%	DCM, 40%	54.6	4.1	47.7±4.3	64
EtAc, 3%	DCM, 40%	59.1	7.4	60.7±3.7	82
DCM, 3%	EtAc, 40%	58.7	10.8	12.9±0.8	23
EtAc, 3%	EtAc, 40%	64.2	13.2	26.2±1.3	46
EtAc, 25%	EtAc, 25%	80.0	3.6	22.7±2.2	69

formed from an EtAc core solution were less uniform than those formed using a DCM core solution. The lowest drug encapsulation efficiencies resulted when EtAc was used in the core solutions (23% and 46% for DCM/EtAc and EtAc/EtAc, respectively), although the drug loading in the EtAc cores was only 10% w/w piroxicam compared to 20% w/w with the DCM cores. The EtAc/DCM sample had the highest drug e.e. (82% w/w).

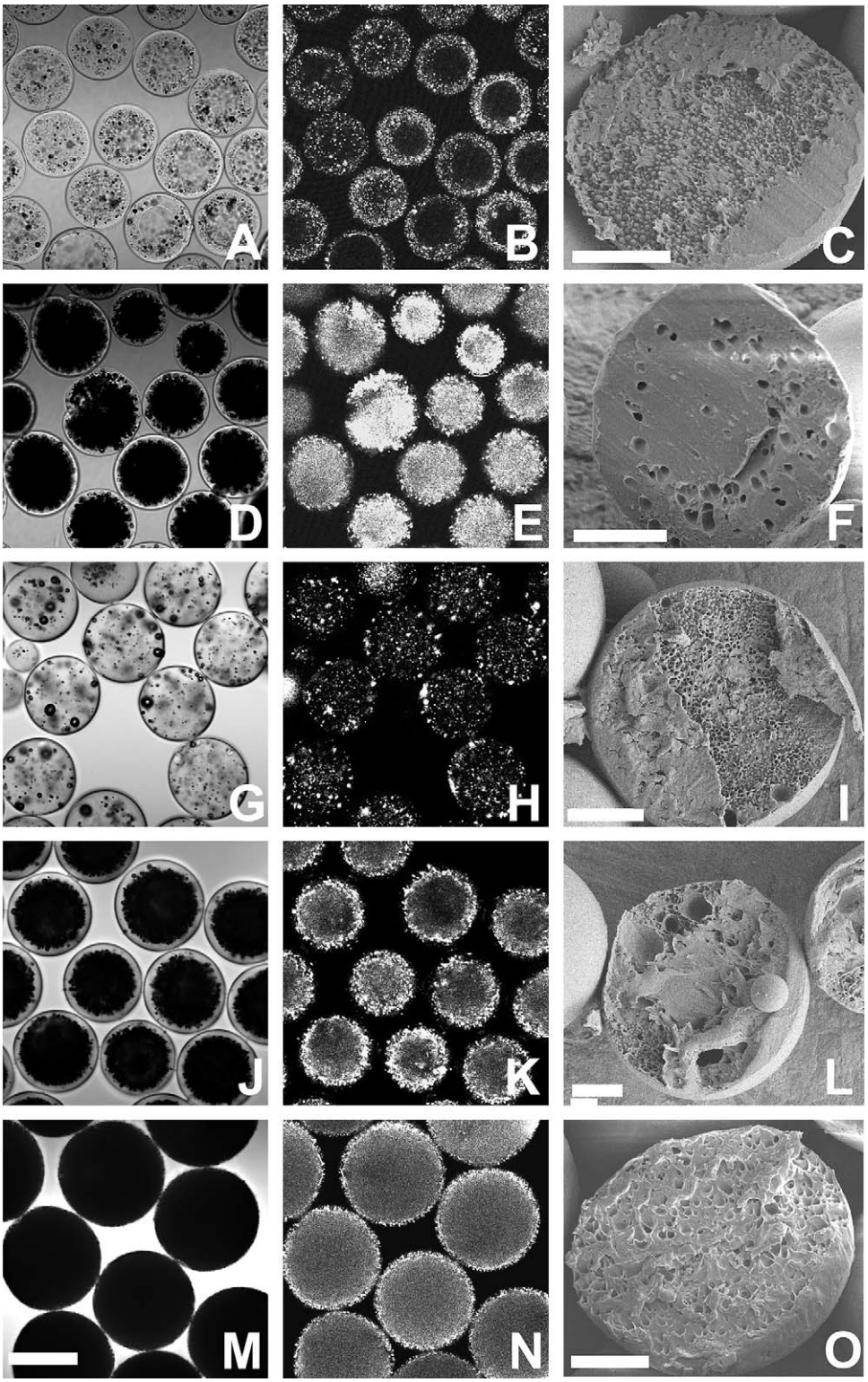

Fig. 2. Optical (first column), fluorescent confocal (second column) and scanning electron (third column) micrographs of piroxicam-loaded PLF(PLG) DWMS fabricated from DCM and EtAc solvents. (A–C) DCM/DCM; (D–F) EtAc/DCM; (G–I) DCM/EtAc; (J–L) EtAc/EtAc (3/40% w/v) and (M–O) EtAc/EtAc (25/25% w/v). Confocal scale bar is 50 μm, SEM scale bars (C, F, I and L) are 15 μm; (O) is 20 μm.

The DWMS prepared from 25% w/v EtAc solutions were 80 μm in diameter—slightly larger than the DWMS fabricated with 3% and 40% shell and core solutions. At 25% w/v the PLF–EtAc solution was quite viscous, even more so than a 40% w/v PLG solution. The increased particle diameter may be due to the actual mass ratios being slightly higher than experimentally set, if the viscosity of the PLF/EtAc solution is enough to "pull" itself at a rate faster than the pump setting. Despite the increased average diameter, the size distribution is relatively uniform. An increase in the drug encapsulation efficiencies from 46% to 69% was observed when using the higher concentration solutions.

In optical micrographs (Fig. 2, left), DWMS made with an EtAc shell solvent show particles generally exhibiting dark centers surrounded by a relatively clear outer ring (for example, Figs. 2D and J). These features are interpreted as representing the desired core–shell morphology. The DCM/EtAc and EtAc/EtAc systems (Figs. 2G and J, respectively) produced less uniform particles while the 25% EtAc/EtAc system (Fig. 2M produced uniform but larger diameters as compared to the DCM/DCM or EtAc/DCM systems (Table 4). Core encapsulation efficiencies could not be calculated for all the samples, as dark regions in the optical images of the lyophilized spheres obscured the interior structures in the EtAc/EtAc sample. The other three samples were determined to have core encapsulations of 56% (DCM/DCM), 92% (EtAc/DCM) and 33% (DCM/EtAc). The EtAc/DCM system resulted in the highest core encapsulation and gave a great improvement on the single DCM/DCM solvent configuration, as predicted by spreading coefficient theory. DCM/EtAc is likewise the least encapsulated, as predicted, although it is unclear whether the polymers had sufficient time before hardening to reverse locations as predicted by the spreading calculations.

Confocal fluorescence micrographs of DCM/DCM particles (Fig. 2B) show a preferential drug distribution to a region near the surface of the particles, while EtAc/DCM and EtAc/EtAc particles (Figs. 2E and K) show localization to the particle interior. (Dark regions exist between the particles in Figs. 2E and K, but the optical images show the particles to be touching, indicating the presence of a drug-free shell.) Fluorescence micrographs of the DWMS prepared from solutions above the critical polymer concentration (Fig. 2N) show a relatively uniform drug distribution with stronger fluorescence near the outer edges of the particles, which may represent the presence of a shell.

SEM images of the cross-sectioned spheres appear to show a core–shell structure for some of the samples (Fig. 2, right). The EtAc/DCM (Fig. 2F) and EtAc/EtAc (Fig. 2L) systems produced particles showing a more porous region toward the particle surface with a denser interior. This porosity could result simply from the faster extraction of the shell solvent or could be due to the core solvent creating channels through which to escape a (partially) hardened shell. Further, polymer–polymer miscibility within the shell phase does not seem to be as prevalent with the EtAc shell, although it is especially noticeable through the entire cross-section of the DCM/DCM sample (compare Figs. 2C and F), in the form of small spheres, presumably of one polymer dispersed in a continuous phase of the other. It is unclear which polymer is the dispersed phase and which is the continuous phase. In the case of the particles exhibiting core–shell morphologies there may exist a continuous region of each polymer (in either the core or shell) with some small amount of the second polymer dispersed in that phase.

5. Conclusions

Thermodynamic parameters have a range of applicability in rational DWMS formation and characterization. Formation of well-defined core–shell particles directly relies on total polymer–polymer immiscibility and preferential spreading of the shell material on the core. Calculations of equilibrium thermodynamic parameters for polymer miscibility, drug distribution and polymer spreading were evaluated through experimental formation of DWMS. Utilizing a fast extracting EtAc shell with a DCM core resulted in the highest drug loadings and core encapsulations efficiencies, as predicted by the preference of piroxicam for the PLG core phase and high λ_{31} value for spreading of PLF on PLG. The high drug loadings found with EtAc/DCM system corresponded to the increased thermodynamic affinity of piroxicam for the PLG in DCM solution. Both the EtAc/DCM and EtAc/EtAc solvent combinations show piroxicam localization to the core, as predicted. The DCM/DCM DWMS, on the other hand, have piroxicam primarily present in the shell, the one deviation from the thermodynamic predictions. The highest core encapsulation is found for the EtAc/DCM sample, also in direct agreement with prediction of strong PLF spreading on PLG with the EtAc/DCM solvent configuration. The ability to predict solvents and polymer concentrations that lead to well-formed microcapsules with desired morphologies may facilitate design of DWMS as controlled release systems.

Acknowledgments

This work was supported by NIH Grant 1-R21-EB002878. We thank Prof. Kevin Kim for use of the PPF apparatus used in production of all particles reported herein. The gifts of piroxicam from Dong Wha Pharmaceuticals and PLF from Guilford Pharmaceuticals are also gratefully acknowledged. Scanning electron microscopy was carried out at the Center for Microanalysis of Materials, University of Illinois at Urbana-Champaign, which is partially supported by the US Department of Energy under Grant DEFG02-91-ER45439.

References

[1] Lambert WJ, Peck KD. Development of an in situ forming biodegradable poly lactide-*co*-glycolide system for the controlled release of proteins. J Control Release 1995;33:189–95.

[2] Loxley A, Vincent B. Preparation of poly(methylmethacrylate) microcapsules with liquid cores. J Colloid Interface Sci 1998;208:49–62.

[3] Sanchez A, Gupta RK, Alonso MJ, Siber GR, Langer R. Pulsed controlled-release system for potential use in vaccine delivery. J Pharm Sci 1996;85:547–52.

[4] Uno K, Ohara Y, Arakawa M, Kondo T. A new method of preparing monocored water-loaded microcapsules using interfacial polymer deposition process. J Microencapsulation 1984;1:3–8.

[5] Watnasirichaikul S, Davies NM, Rades T, Tucker IG. Preparation of biodegradable insulin nanocapsules from biocompatible microemulsions. Pharm Res 2000;17:684–9.

[6] Leach KJ, Mathiowitz E. Degradation of double-walled polymer microspheres of PLLA and P(CPP:SA)20:80. I. In vitro degradation. Biomaterials 1998;19:1973–80.

[7] Lee TH, Wang J, Wang C-H. Double-walled microspheres for the sustained release of a highly water soluble drug: characterization and irradiation studies. J Control Release 2002;83:437–52.

[8] Pekarek KJ, Jacob JS, Mathiowitz E. One-step preparation of double-walled microspheres. Adv Mater 1994;6:684–7.

[9] Yang Y-Y, Shi M, Goh S-H, Moochhala SM, Ng S, Heller J. POE/PLGA composite microspheres: formation and in vitro behavior of double walled microspheres. J Control Release 2003;88:201–13.

[10] Berkland C, Pollauf E, Pack DW, Kim K. Uniform double-walled polymer microspheres of controllable shell thickness. J Control Release 2004;96:101–11.

[11] Rahman NA, Mathiowitz E. Localization of bovine serum albumin in doublewalled microspheres. J Control Release 2004;94:163–75.

[12] Shi M, Yang Y-Y, Chaw C- S, Goh S-H, Moochhala SM, Ng S, et al. Double walled POE/PLGA microspheres: encapsulation of water-soluble and water-insoluble proteins and their release properties. J Control Release 2003;89:167–77.

[13] Pekarek KJ, Jacob JS, Mathiowitz E. Double-walled polymer microspheres for controlled drug release. Nature 1994;367:258–60.

[14] Pekarek KJ, Dyrud MJ, Ferrer K, Jong YS, Mathiowitz E. In vitro and in vivo degradation of double-walled polymer microspheres. J Control Release 1996;40:169–78.

[15] Berkland C, Cox A, Kim KK, Pack DW. Three-month, zero-order piroxicam release from monodispersed double-walled microspheres of controlled shell thickness. J Biomed Mater Res 2004;70A:576–84.

[16] Pollauf E, Kim KK, Pack DW. Small-molecule release from poly(d,l-lactide)/poly(d,l-lactide-co-glycolide) composite microparticles. J Pharm Sci 2005;94:2013–22.

[17] Harkins WD. The physical chemistry of surface films. New York: Reinhold; 1952.

[18] Matsumoto A, Matsukawa Y, Suzuki T, Yoshino H, Kobayashi M. The polymer-alloys method as a new preparation method of biodegradable microspheres: principle and application to cisplatin-loaded microspheres. J Control Release 1997;48:19–27.

[19] Gopferich A, Alonso MJ, Langer R. Development and characterization of microencapsulated microspheres. Pharm Res 1994;11:1568–74.

[20] Leach KJ, Takahashi S, Mathiowitz E. Degradation of double-walled polymer microspheres of PLLA and P(CPP:SA)20:80. II. In vivo degradation. Biomaterials 1998;19:1981–8.

[21] Berkland C, Kim K, Pack DW. Fabrication of PLG microspheres with precisely controlled and monodisperse size distributions. J Control Release 2001;73:59–74.

[22] Berkland C, King M, Cox A, Kim K, Pack DW. Precise control of PLG microsphere size provides enhanced control of drug release rate. J Control Release 2002;82:137–47.

[23] Pollauf EJ, Berkland C, Kim KK, Pack DW. In vitro degradation of polyanhydride/polyester core–shell double-wall microspheres. Int J Pharm 2005;301:294–303.

[24] Hildebrand JH, Scott RL. The solubility of nonelectrolytes. New York: Reinhold; 1950.

[25] Hansen CM. Hansen solubility parameters: a user's handbook. Boca Raton: CRC Press; 2000.

[26] van Krevelen DW. Properties of polymers: their estimation and correlation with chemical structure. 2nd ed. Amsterdam: Elsevier; 1976.

[27] Fedors RF. A method for estimating both the solubility parameters and molar volumes of liquids. Polym Eng Sci 1974;14:147–54.

[28] Flory PJ. Principles of polymer chemistry. Ithaca, NY: Cornell University Press; 1953.

[29] Scott RL. The thermodynamics of high polymer solutions. V. Phase equilibria in the ternary system: polymer 1–polymer 2–solvent. J Chem Phys 1949;17:279–84.

[30] Scott RL. The thermodynamics of high polymer solutions. IV. Phase equilibria in the ternary system: polymer–liquid 1–liquid 2. J Chem Phys 1949;17:268–79.

[31] Snyder LR. The role of the mobile phase in liquid chromatography. In: Kirkland JJ, editor. Modern practice of liquid chromatography. New York: Wiley; 1971.

[32] Torza S, Mason SG. Three-phase interactions in shear and electrical fields. J Colloid Interface Sci 1970;33:67–83.

[33] Hobbs SY, Dekkers MEJ, Watkins VH. Effect of interfacial forces on polymer blend morphologies. Polymer 1988;29:1598–602.

[34] Wu S. Polymer interface and adhesion. New York: Marcel-Dekker; 1982.

[35] Zhao Z, Chaubal M, Su G, Jiang T, Dang W. In vitro degradation studies of polilactofates—a copolymer of lactide and phosphate. Int Symp Control Release Bioactive Mater 2000;27:652–3.

[36] Park TG. Degradation of poly(lactic-*co*-glycolic acid) microspheres: effect of copolymer composition. Biomaterials 1995;16:1123–30.

[37] Bustamante P, Pena MA, Barra J. Partial solubility parameters of piroxicam and niumic acid. Int J Pharm 1998;174:141–50.

[38] Grulke EA. Solubility parameter values. In: Brandrup J, Immergut EH, editors. Polymer handbook. 3rd ed. New York: Wiley; 1989. p. 519–59.

[39] Meng FT, Ma GHM, Qui W, Su ZG. W/O/W double emulsion technique using ethyl acetate as organic solvent: effects of its diffusion rate on the characteristics of microparticles. J Control Release 2003;91:407–16.